On the time-fractional Schrödinger equation: theoretical analysis and numerical solution by matrix Mittag–Leffler functions*

Roberto Garrappa
Università degli Studi di Bari, Dipartimento di Matematica, Bari, Italy
roberto.garrappa@uniba.it

Igor Moret
Università degli Studi di Trieste, Dipartimento di Matematica e Geoscienze, Trieste, Italy
moret@units.it

Marina Popolizio†
Università del Salento, Dipartimento di Matematica e Fisica "Ennio De Giorgi", Lecce, Italy
marina.popolizio@unisalento.it

Abstract

This paper presents an original analysis of a time-dependent Schrödinger equation with fractional time derivative. After the discretization of the spatial operator the equation is reformulated in terms of a special system of fractional differential equations; it occurs that the eigenvalues of the coefficient matrix lay on the boundary of the stability region of fractional differential equations. The main difficulties in solving this system are hence related to the simultaneous presence of persisting oscillations (possibly with high frequency as it is typical with Schrödinger equations) and a persisting memory (as a consequence of the fractional order); moreover, an accurate spatial discretization gives rise to systems of large to very large size, involving a noteworthy computational complexity. By means of a theoretical analysis the exact solution is split into two or three terms (depending on the order of the fractional derivative), thus to face the numerical computation by different and suitably selected methods: direct evaluation of matrix functions for the terms characterized by smooth behaviour but with persistent memory and a step-by-step strategy, in conjunction with matrix function, for the oscillating term. In both cases, Krylov subspace methods are employed for the computation of matrix functions and convergence results are presented.

Keywords: Time–fractional Schrödinger equation, Mittag–Leffler function, Krylov subspace methods, shift-and-invert, convergence

*Preprint of a paper which will be published in "Computers & Mathematics with Applications', doi: 10.1016/j.camwa.2016.11.028. Work supported under the GNCS - INdAM Project 2016.

†Corresponding author

1 Introduction

The time-dependent Schrödinger equation describes the evolution of the wave function of a single non-relativistic particle and can be viewed as the analogue, in quantum physics, of the classic Newton's second law. Recently this fundamental equation has been reformulated in a more general setting by replacing the standard integer-order derivative by a derivative of non-integer order.

A first generalization of the Schrödinger equation to fractional-space derivatives was proposed by Laskin in 2000 [1] to provide a fractional approach for the quantum chromodynamics problem of quarkonium. Successively, in 2004 Mark G. Naber [2] reformulated the time-dependent Schrödinger equation by replacing the integer-order time-derivative with the fractional derivative introduced by Caputo (see [3]).

These generalizations are common to many fundamental equations of physics since fractional order derivatives turn out to be more suitable for describing anomalous behaviours frequently observed in complex systems. In particular, due to their non-local character, fractional integrals and fractional derivatives constitute valuable tools for introducing, in mathematical models, hereditary and non-Markovian effects which are typical of heterogeneous systems.

We recognize that fractional Schrödinger equations still not have a completely clear physical meaning or, worse, in some generalizations questionable models are derived, as shown in [4] for some space–fractional versions. For the time–fractional Schrödinger equations (TFSEs) the non–Markovian evolution can be the key for a theoretical reading, while, from a computational point of view, their solution is a highly challenging and stimulating problem. For this reason we think that the analysis and the development of numerical methods for TFSEs are surely of interest, also due to the difficulties of finding analytical solutions. Moreover, developing strategies to get suitable numerical approximations of TFSEs can give a hint to tackle other likewise challenging problems.

Actually, Naber derived two TFSEs roughly differing by the complex coefficient of the fractional derivative. Most of the works so far presented in the literature deal with the first of these two equations, the one with the coefficient proportional to the imaginary unit i, and nowadays several methods for the numerical solution of this problem have been analysed (e.g., see [5, 6, 7, 8, 9, 10, 11]).

The second equation proposed by Naber was obtained after performing a Wick rotation and, if α represents the time–derivative order, a coefficient i^α, instead of i, results in the equation; this formulation is considered robust since the temporal behaviour of the solution preserves the sustained oscillations which are instead lost in the first formulation. However, its numerical treatment is considerably more difficult because of the simultaneous presence of persistent oscillations and memory preservation. In this paper we examine this issue fully.

As in our previous paper [12], we are interested in exploiting effective well–established methods for the computation of matrix functions combined with competitive integrators for differential equations. Methods of this kind are usually known under the name of *exponential integrators* for the key role played by the exponential function; they have been extensively studied for integer ordinary differential equations (ODEs) (e.g., [13, 14, 15, 16, 17, 18, 19, 20]), also for the Schrödinger equations [21, 22, 23]. In particular, when the matrix arises from the discretization of spatial operators, and hence presents sparsity and large size, methods based on the Krylov subspaces appear suitable to keep the computation at an affordable level.

Recently the application of exponential integrators has been successfully extended and investigated also for fractional order problems [24, 25]; a major feature is that here the

exponential function is replaced by the more involved Mittag–Leffler (ML) function.

As already discussed in [12], approximating the ML function with matrix arguments arising in the numerical treatment of TFSEs can be extremely difficult. A thorough theoretical analysis of the ML function in this context can however reveal useful information to be used for devising ad-hoc computational strategies. It is indeed possible to distinguish two main terms: the first term is non-local but not oscillatory and hence it appears suitable to be handled by approximating matrix functions with Krylov subspace methods. The second term is instead highly oscillatory but of local nature; indeed it can be re-conducted to a problem of integer order and it can therefore be treated in a step-by-step way again by technique of exponential type (possibly grounded on Krylov subspace methods) or by a finite difference method suitably chosen in order to preserve the perfect oscillating behaviour.

We must also mention an additional specific feature of TFSEs consisting in the dependence on the fractional order α of the dynamics and the oscillating frequency of the solution; it is obvious that this is a source of new and non trivial computational difficulties since it is sometimes necessary to modify the numerical approach according to the value of the fractional order α.

It is therefore necessary to study this problem in a comprehensive way and try to extract as much information as possible on the exact solution in order to devise the most suitable approaches with respect to the order α; in this sense, and just for completeness of presentation, this work includes also some of the results presented in [12] for the case $0 < \alpha < 1$.

The structure of this paper is the following. In the next section we recall some basics about fractional derivatives, we introduce the TFSE and we provide a representation of its exact solution. In Section 3 we briefly review Krylov subspace methods and their use for the approximation of matrix functions. Section 4 is devoted to study the ML function and, in particular, to identify the different terms constituting this function when applied to the arguments involved in the discretization of the TFSE; besides, we discuss the more qualified numerical approaches to approximate each term. The qualitative results described in this section are studied under a more technical point of view in Section 5; there we investigate the convergence properties of Krylov subspace methods and their dependency on the parameters of the ML function and on the characteristics of the argument A (to facilitate the reading, all the proofs of the technical results on convergence are collected in Appendix at the end of the paper). Although numerical simulations go with theoretical results throughout the whole paper, some final experiments are presented in Section 6.

2 Fractional derivatives and time-fractional Schrödinger equation

To introduce the problem under investigation we preliminarily recall some basic concepts in fractional calculus. In particular we start from the definition of the Riemann-Liouville (RL) integral of real order $\alpha > 0$ which for a function $f \in L^1([0,T])$ is given by

$$ {}_0J_t^\alpha f(t) = \frac{1}{\Gamma(\alpha)} \int_0^t (t-u)^{\alpha-1} f(u)\,\mathrm{d}u, \quad t \in [0,T], $$

where $\Gamma(z)$ is the Euler gamma function. Fractional derivative operators for inverting the RL integral can be introduced according to different approaches. In this paper we are

interested in the Caputo's fractional derivative

$$ {}_0D_t^\alpha f(t) \equiv {}_0J_t^{m-\alpha} f^{(m)}(t) = \frac{1}{\Gamma(m-\alpha)} \int_0^t (t-u)^{m-\alpha-1} f^{(m)}(u)\,\mathrm{d}u, $$

where m is the smallest integer such that $m > \alpha$ and $f^{(m)}$ denotes the standard integer-order derivative (for obvious reasons f is assumed to be an m-times absolutely continuous function). We refer to [3, 26, 27, 28] for background material on fractional calculus.

For a non-relativistic particle, with mass $\hat{m}$ and potential energy $V(x)$, Naber [2] proposed the following TFSE

$$ \mathrm{i}^\alpha \hbar T_p^{1-\alpha} {}_0D_t^\alpha \psi = -\frac{\hbar^2}{2\hat{m}} \nabla_x^2 \psi + V(x)\psi, \tag{1} $$

where $\psi = \psi(t,x)$ is the position-space wavefunction of the particle in a multidimensional domain $\Omega \subseteq \mathbb{R}^d$, ∇_x^2 the spatial Laplacian operator, $\mathrm{i} = \sqrt{-1}$ the imaginary unit, $\hbar$ the reduced Planck's constant and T_p the Planck time. The above equation is closed by a proper choice of initial and boundary conditions whose number and form depend also on the fractional order α. Here we assume $0 < \alpha < 2$, as it usually is in the most common applications. As a matter of fact, the case α close to 1 deserves usually more attention.

For practical computation, a spatial discretization scheme is employed to replace the infinite dimensional operator ∇_x^2 with a finite dimensional linear operator (namely a matrix), thus to recast the original TFSE (1) into a system of fractional differential equations (FDEs)

$$ {}_0D_t^\alpha y(t) = (-\mathrm{i})^\alpha A y(t) + b \tag{2} $$

coupled with standard initial conditions of Cauchy type

$$ \begin{cases} y(0) = y_0 & 0 < \alpha \le 1 \\ y(0) = y_0,\ y'(0) = y_0' & 1 < \alpha < 2 \end{cases}, $$

and where the vector b collects contributions from boundary conditions. The matrix A is symmetric and positive definite, usually with a sparse pattern. Depending on the dimension of the domain Ω and on the refinement of the spatial discretization, the size N of the system (2) can be exceedingly large (it is quite common to deal with thousands up to millions equations). The development of efficient methods is therefore of primary importance to numerically solve (2).

Independently from the original TFSE from which it is derived, system (2) is also of interest as a model problem possessing the spectrum on the boundary of the region of stability for FDEs, namely $\{z \in \mathbb{C} : |\arg(z)| \ge \alpha\pi/2\}$.

As in the integer-order case, the numerical treatment of problems of this kind is a non trivial task and, as far as we know, this issue has not been properly addressed in the context of fractional calculus.

Because of the nonlocal nature of fractional operators, finite difference methods demand the storage and the use of the whole history of the solution. Indeed, unlike differential equations of integer order, for FDEs it is not possible to apply a step-by-step approach allowing to express the solution in terms of the solution in one of just few previous time-steps. Thus the numerical evaluation of the solution at each time-step involves the use of the whole sequence of approximations in all the previous time-steps.

This issue can be a critical problem not only from the computational point of view (due to large storage and high cpu time) but it can also represent a source of numerical instability. Round-off errors, indeed, accumulate and propagate in long calculations

(especially when the integration is required on large intervals or with small step-sizes); this can lead to catastrophic cancellation with the consequence that the behaviour of the numerical solution deviates from that of the exact solution which, as we will discuss later, is highly oscillatory.

It is well-known (e.g., see [26, 27, 28]) that the exact solution of (2) can be expressed as

$$y(t) = \begin{cases} e_{\alpha,1}(t; (-\mathrm{i})^\alpha A)y_0 + e_{\alpha,\alpha}(t; (-\mathrm{i})^\alpha A)b & 0 < \alpha \leq 1 \\ e_{\alpha,1}(t; (-\mathrm{i})^\alpha A)y_0 + e_{\alpha,2}(t; (-\mathrm{i})^\alpha A)y_0' + e_{\alpha,\alpha}(t; (-\mathrm{i})^\alpha A)b & 1 < \alpha < 2 \end{cases} \tag{3}$$

where the function $e_{\alpha,\beta}(t; z) = t^{\beta-1}E_{\alpha,\beta}(t^\alpha z)$ is a generalization of the two parameter ML function [29, 26, 27, 28]

$$E_{\alpha,\beta}(z) = \sum_{k=0}^{\infty} \frac{z^k}{\Gamma(\alpha k + \beta)}, \quad z \in \mathbb{C}, \quad \alpha, \beta \in \mathbb{C}, \quad \Re(\alpha) > 0.$$

Equations like (3) were considered in the past just as a theoretical tool for expressing the analytical solution of the system because of the presence of matrix functions with large arguments; only the quite recent introduction of reliable methods tailored to this purpose allowed the development of exponential integrators for solving ODEs, successively generalized also to FDEs.

The strength of this strategy is that in several cases it is possible to evaluate the solution directly at a given time, without computing, storing and using the whole history. This provides substantial computational advantages especially with problems of large size and in the presence of a persistent memory as in fractional order problems.

3 Approximation of matrix functions by Krylov subspace methods

A determining aspect for the competitiveness of exponential integrators is the computation of the action of matrix functions on vectors. Indeed, as said in Section 2, the starting point of these methods is the formulation of the solution in these terms. We just refer to [30] and references therein for a complete treatise on matrix functions, both for theoretical and practical aspects. Specifically, in our case the solution (3) of the TFSE (1) involves the evaluation of vectors like $e_{\alpha,\beta}(A)v$, for given matrices A and vectors v. This computation becomes thus decisive since in general the matrix arguments are very large and a naïve implementation would frustrate any advantage of the method. The Krylov subspace methods are currently among the most effective approaches for this goal and their effectiveness in approximating the ML function has been recently addressed [31, 32, 12]. We thus make use of Krylov subspace methods for our purposes and we introduce them by referring to a generic well–defined function f.

The basic idea of the standard polynomial Krylov method (SKM) is to approximate $f(A)v$ in the Krylov subspaces

$$\mathcal{K}_m(A, v) = \mathrm{span}\{v, Av, A^2v, \ldots, A^{m-1}v\}, \ m \in \mathbb{N}.$$

The Arnoldi method is usually used to work with these spaces. It starts from the initial vector $v_1 = v/\|v\|$, builds an orthonormal basis $\{v_1, v_2, \ldots, v_m\}$ of $\mathcal{K}_m(A, v)$ and stores it as the columns of a matrix $V_m = [v_1, v_2, \ldots, v_m]$. The process gives rise also to a matrix $H_{m+1,m}$ which collects the coefficients $h_{i,j}$ of the Gram-Schmitd orthonormalization of

each v_i against all the previous basis vectors. This is an $m+1 \times m$ upper–Hessenberg matrix and we denote with H_m the matrix obtained by deleting the last row in $H_{m+1,m}$. Then

$$V_m^T A V_m = H_m$$

and the following Arnoldi relation holds

$$AV_m = V_m H_m + \|v\| h_{m+1,m} v_{m+1} e_m^T$$

with $e_m = [0, \ldots, 0, 1]^T \in \mathbb{R}^m$. Theoretically one would stop the procedure when $h_{m+1,m}$ vanishes since the corresponding Krylov subspace $\mathcal{K}_m(A, v)$ would be invariant under A and thus an approximation in this space would be exact. In practice this is not a practical way to choose the projection space but monitoring the quantity $\|h_{m+1,m} v_{m+1}\|$ could be a strategy. Then the consequent approximation is

$$f(A)v \approx \|v\| V_m f(H_m) e_1 \tag{4}$$

with $e_1 = [1, 0, \ldots, 0]^T \in \mathbb{R}^m$. This approximation basically requires to evaluate f on a matrix smaller than A and then expand back the result. The procedure is clearly effective when $m \ll N$ since general purpose methods are usually at disposal to compute $f(H_m)$ for small matrix arguments H_m.

Useful insights come from looking at the approximation (4) as the polynomial interpolation, in the Hermite sense, of f on the eigenvalues of H_m (also known as the *Ritz values* of A) repeated according to their multiplicities. We report this interesting result due to a pioneering work by Saad [33].

Theorem 3.1. *Let V_m, H_m be the result of m steps of the Arnoldi process on $A \in \mathbb{C}^{N \times N}$ and $v \in \mathbb{C}^N$. Then*

$$\|v\| V_m f(H_m) e_1 = \tilde{p}_{m-1}(A) v$$

where $\tilde{p}_{m-1}$ is the unique polynomial of degree at most $m-1$ that interpolates f on the spectrum of H_m.

We point out that we are actually interested in complex matrix arguments of the form $(-\mathrm{i})^\alpha t^\alpha A$ but fortunately, for the invariance properties of Krylov subspaces, these are constructed handling only the real matrix A, while complex arithmetic is involved only in the evaluation of scalar terms when computing $f((-\mathrm{i})^\alpha t^\alpha H_m)$.

It is worthwhile to note that the dimension of the Krylov subspace is fundamental for the efficiency of the numerical approach. Indeed, not only producing spaces of large dimension can be computationally expensive, but the evaluation of the matrix function can become prohibitive on projection spaces of large dimension.

As it is well known, the convergence of Krylov subspace methods strongly depends on the spectrum of A and it degenerates as the convex hull of the spectrum enlarges. We refer to [31] for a discussion of this topic in the case of ML functions as well as for related references.

To overcome this difficulty the *shift-and-invert* Krylov method (SIKM) was introduced in [34], and later in [35], to get a faster convergence. It actually belongs to the class of *rational* Krylov methods when just one pole is used. In this case the Krylov subspaces are generated by

$$Z = (\delta I + A)^{-1}$$

for a suitably chosen real scalar $\delta > 0$. The corresponding approximation is

$$f(A)v \approx \|v\| U_m f(\tilde{H}_m) e_1$$

with $\tilde{H}_m = H_m^{-1} - \delta I$, H_m denoting the Hessenberg reduction of Z, $U_m = [u_1, \ldots, u_m]$ with $u_1 = v/\|v\|$ and $u_1, \ldots, u_m$ orthonormal vectors. Each step of the SIKM is more expensive than one of SKM since a linear system with coefficient matrix Z is required and finally the inversion of H_m is needed to get the final approximation. For the first task direct or iterative solvers could be applied: in both cases a reduction of the computational effort is possible since a factorization, for the former, or a preconditioner, for the latter, can be computed just once at the beginning of the process. However, in general the fast convergence of SIKM legitimizes this additional entanglement.

Also this approximation can be seen as a polynomial interpolation of f in the eigenvalues of $\tilde{H}_m$. Anyhow, we will return later on this point showing some numerical comparisons between SKM and SIKM.

Remark 3.2. *When A denotes an infinite dimensional operator the SIKM can be quietly applied while SKM can be applied only if v is in the domain of A and its successive powers.*

We can test the efficiency of SKM and SIKM for the numerical solution of the system (2) stemming from the semi–discretization, along only the space variables, of problem (1). We consider the same 2D problem described in Section 6; we apply standard finite differences on a mesh-grid of 50 points along each dimension, thus resulting in a matrix A of size $2,500 \times 2,500$. The solution thus requires the computation of $e_{\alpha,1}(t; (-\mathrm{i})^\alpha A)v$ and/or $e_{\alpha,2}(t; (-\mathrm{i})^\alpha A)v$ when $\alpha > 1$. We then apply SKM and SIKM for the evaluation of these terms for different values of α. Different shift parameters are considered for SIKM in order to analyse the influence of this factor on the method's performance. As reference solution we compute $e_{\alpha,\beta}(t; (-\mathrm{i})^\alpha A)$, for $\beta = 1, 2$, by combining the `funm` Matlab routine and the `ml` code devised in [36]. We do the same for $e_{\alpha,\beta}(t; (-\mathrm{i})^\alpha H_m)$ with H_m denoting the Hessenberg projections into the appropriate Krylov spaces.

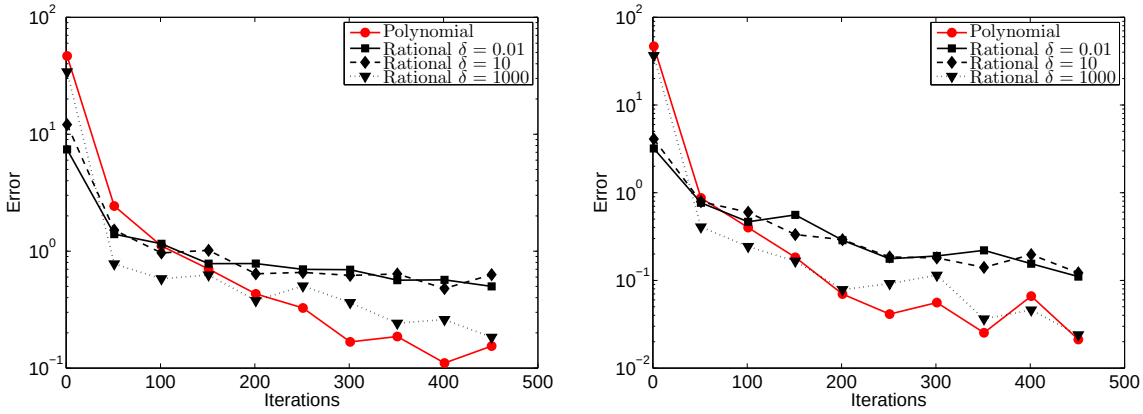

Figure 1: Errors by polynomial (SKM) and rational (SIKM) Krylov methods for $e_{\alpha,1}(t; (-\mathrm{i})^\alpha A)v$ for the 2D problem ($N = 2,500$) at $t = 1$; $\alpha = 0.7$ (left plot) and $\alpha = 0.9$ (right plot).

Figures 1-2 show that Krylov subspace methods fail in approximating $e_{\alpha,\beta}(t; (-\mathrm{i})^\alpha A)v$ since, even in very large spaces, the computed approximation is quite far from the exact solution. No advantage is gained by using SIKM either, regardless of the choice of the shift parameter. This odd phenomenon has inspired the deeper analysis that we are going to address in the following sections. In fact, we derive a split of the exact solution which enables us to optimally use the Krylov subspace methods on each part. In this way the required accuracy is always reached.

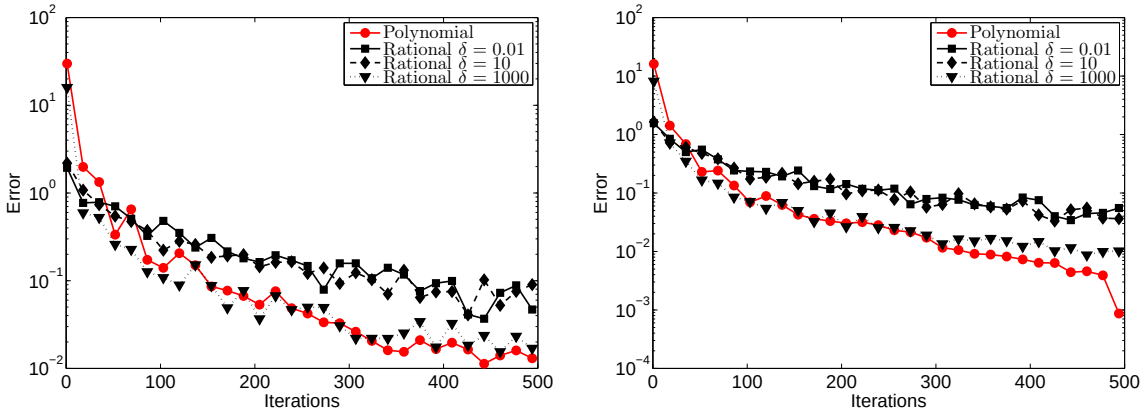

Figure 2: Errors by polynomial (SKM) and rational (SIKM) Krylov methods for $e_{\alpha,2}(t;(-\mathrm{i})^\alpha A)v$ for the 2D problem ($N = 2,500$) at $t = 1$; $\alpha = 1.1$ (left plot) and $\alpha = 1.3$ (right plot).

4 The Mittag–Leffler function: integral formulations and properties

The ML function $E_{\alpha,\beta}$ and its generalization $e_{\alpha,\beta}$ play a crucial role in the analysis and solution of FDEs. It is hence of fundamental importance to investigate their main properties and the techniques available for their numerical computation, also with matrix arguments.

4.1 Laplace transform and integral formulations

One of the most powerful tools for the analysis and computation of several special functions is the Laplace transform (LT). This is also the case of the generalized ML function $e_{\alpha,\beta}(t;z)$ whose LT is [28, 27]

$$\mathcal{E}_{\alpha,\beta}(s;z) \equiv \mathcal{L}(e_{\alpha,\beta}(t;z)\,;\,s) = \frac{s^{\alpha-\beta}}{s^\alpha - z}, \quad \Re(s) > 0 \ \text{ and } \ |zs^{-\alpha}| < 1\,,$$

(as a consequence of the presence of real powers, $\mathcal{E}_{\alpha,\beta}(s;z)$ is a multi-valued function and, hence, a branch cut is required on the complex plane which, for convenience, is placed along the negative real axis $(-\infty, 0]$). By the inversion formula of the LT it is therefore possible to represent $e_{\alpha,\beta}(t;z)$ by the integral formulation

$$e_{\alpha,\beta}(t;z) = \frac{1}{2\pi\mathrm{i}} \int_{\mathcal{C}} \mathrm{e}^{st} \mathcal{E}_{\alpha,\beta}(s;z)\,\mathrm{d}s, \tag{5}$$

where $\mathcal{C}$ is a suitable deformation of the Bromwich line chosen in order to encompass all the singularities of $\mathcal{E}_{\alpha,\beta}(s;\lambda)$.

The solution of (1) involves terms like $e_{\alpha,\beta}(t;z)$ with $z = (-\mathrm{i})^\alpha\lambda$, for real $\lambda > 0$. To describe the qualitative behaviour of these terms we make use of *completely monotonic* functions.

Definition 4.1. *A function $f : (0,+\infty) \to \mathbb{R}$ is said completely monotonic (c.m.) on $(0,+\infty)$ if f has derivatives of all orders and $(-1)^k f^{(k)}(t) \geq 0$ for any $k \in \mathbb{N}$ and $t > 0$.*

Since the limits as $t \to 0$ of $f^{(k)}(t)$ exist, the c.m. function can be extended to $[0,\infty)$ when these limits are finite. A well-known result, usually referred to as the Bernstein's

theorem [37, page 160], states that a function f is c.m. on $[0,+\infty)$ if and only if it is the LT of a finite non-negative Borel measure on $[0,+\infty)$. In other words, there must exist a distribution function $K(r) \geq 0$, $r \geq 0$, such that $f(t)$ can be written as

$$f(t) = \int_0^t \mathrm{e}^{-rt} K(r)\,\mathrm{d}r.$$

For our analysis, c.m. functions are of particular interest since they have an extremely regular behaviour; unlike high-frequency oscillating functions, it is indeed quite easy to approximate c.m. functions by means, for instance, of polynomials or rational functions.

To study and approximate ML functions it is therefore of some help to clearly identify the contribution of regular (in this case c.m.) and less regular (oscillating) terms; the aim is to treat each term in the most appropriate way according to the expected behaviour. We thus provide the following result.

Theorem 4.2. *Let $0 < \alpha < 2$ and $\lambda > 0$ real. Then for any $t > 0$*

$$e_{\alpha,\beta}(t; (-\mathrm{i})^\alpha \lambda) = F_{\alpha,\beta}(t;\lambda) + \frac{1}{\alpha}(-\mathrm{i}\lambda^{1/\alpha})^{1-\beta}\Big(G_\alpha(t;\lambda) + \varphi(\alpha)^{1-\beta} H_\alpha(t;\lambda)\Big),$$

where $F_{\alpha,\beta}(t;\lambda)$ is a linear combination of c.m. functions,

$$G_\alpha(t;\lambda) = \mathrm{e}^{-\mathrm{i}t\lambda^{1/\alpha}}, \quad H_\alpha(t;\lambda) = \begin{cases} 0 & 0 < \alpha \leq \frac{4}{3} \\ \mathrm{e}^{-\mathrm{i}\varphi(\alpha)t\lambda^{1/\alpha}} & \frac{4}{3} < \alpha < 2 \end{cases}$$

and $\varphi(\alpha) = \mathrm{e}^{2\pi i/\alpha}$.

Proof. Denote with S the set of all singularities of the LT of $e_{\alpha,\beta}(t;(-\mathrm{i})^\alpha\lambda)$ except for possible singularities on the branch–cut. This set is obtained by considering the solutions in the main Riemann sheet (i.e., those with the argument in $(-\pi,\pi]$) of $s^\alpha - (-\mathrm{i})^\alpha\lambda = 0$; a direct calculation allows to evaluate

$$S = \begin{cases} \{-\mathrm{i}\lambda^{1/\alpha}\} & 0 < \alpha \leq \frac{4}{3} \\ \{-\mathrm{i}\lambda^{1/\alpha}, -\mathrm{i}\lambda^{1/\alpha}\mathrm{e}^{2\pi\mathrm{i}/\alpha}\} & \frac{4}{3} < \alpha < 2. \end{cases}$$

Deform now the contour $\mathcal{C}$ of the inversion formula (5) into a Hankel contour $\mathcal{H}_\gamma$ starting from $-\infty$, moving below the negative real semi-axis, surrounding the origin in the positive (counterclockwise) sense along a circular disc $|s| = \gamma$ and returning to $-\infty$ above the negative real semi-axis. When $\gamma \to 0$ the contour $\mathcal{H}_\gamma$ crosses the poles of $\mathcal{E}_{\alpha,\beta}$ and, hence, a residue subtraction leads to

$$e_{\alpha,\beta}(t;(-\mathrm{i})^\alpha\lambda) = F_{\alpha,\beta}(t;\lambda) + \sum_{s^\star \in S} Res\big(\mathrm{e}^{st}\mathcal{E}_{\alpha,\beta}(s;(-\mathrm{i})^\alpha\lambda), s^\star\big),$$

where

$$F_{\alpha,\beta}(t;\lambda) = \lim_{\gamma\to 0} \frac{1}{2\pi\mathrm{i}} \int_{\mathcal{H}_\gamma} \mathrm{e}^{st}\mathcal{E}_{\alpha,\beta}(s;(-\mathrm{i})^\alpha\lambda)\,\mathrm{d}s. \tag{6}$$

By integrating (6) in a standard way, after denoting with $F^{\pm}_{\alpha,\gamma}(t;\lambda)$ the real valued function

$$F^{\pm}_{\alpha,\gamma}(t;\lambda) = \int_0^\infty \mathrm{e}^{-rt} \frac{r^{\alpha-\gamma}}{r^{2\alpha} - 2r^\alpha\lambda\cos\left(\alpha\pi \mp \frac{\alpha\pi}{2}\right) + \lambda^2}\,\mathrm{d}r,$$

simple derivations allow to evaluate

$$F_{\alpha,\beta}(t;\lambda) = \frac{1}{2\pi i}\Big[\mathrm{e}^{\beta\pi\mathrm{i}}F^{-}_{\alpha,\beta-\alpha}(t;\lambda) - \lambda\mathrm{e}^{(\beta-\frac{\alpha}{2})\pi\mathrm{i}}F^{-}_{\alpha,\beta}(t;\lambda) + \\ - \mathrm{e}^{-\beta\pi\mathrm{i}}F^{+}_{\alpha,\beta-\alpha}(t;\lambda) + \lambda\mathrm{e}^{(\frac{3\alpha}{2}-\beta)\pi\mathrm{i}}F^{+}_{\alpha,\beta}(t;\lambda)\Big]; \qquad (7)$$

the c.m. character of $F^{\pm}_{\alpha,\gamma}(t;\lambda)$ is then a direct consequence of the aforementioned Bernstein's theorem. The residues of the LT of the ML function can be evaluated in an analytical way; it is indeed immediate to verify that

$$Res\big(\mathrm{e}^{st}\mathcal{E}_{\alpha,\beta}(s;z),s^{\star}\big) = \frac{1}{\alpha}\sum_{s^{\star}\in S}\mathrm{e}^{ts^{\star}}(s^{\star})^{1-\beta}$$

and hence, after defining $s^{\star}_1 = -\mathrm{i}\lambda^{1/\alpha}$ and $s^{\star}_2 = -\mathrm{i}\lambda^{1/\alpha}\mathrm{e}^{2\pi\mathrm{i}/\alpha}$, the proof follows by collecting in $G_{\alpha}(t;\lambda)$ the residue at $s^{\star}_1$ and in $H_{\alpha}(t;\lambda)$ the contribution due to the singularity $s^{\star}_2$ (which exists only when $\frac{4}{3} < \alpha < 2$). □ □

The special structure of $F_{\alpha,\beta}(t;\lambda)$, expressed in (7) as the combination of few c.m. functions, assures that its real and imaginary parts have just a very limited number of extrema points and over long times, i.e. when $t \to \infty$, they decay towards 0. This very smooth behaviour can be appreciated in Figure 3 where $F_{\alpha,\beta}(t;\lambda)$ is plotted for some instances of its parameters.

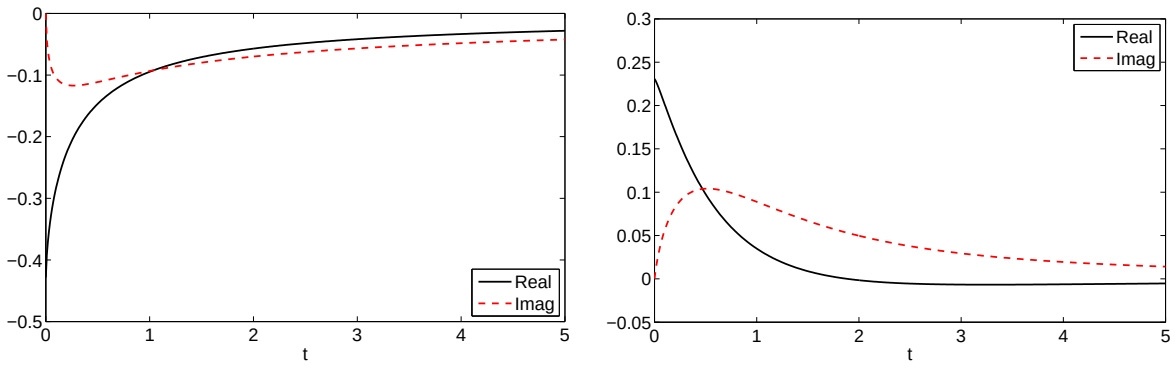

Figure 3: Real and imaginary parts of $F_{\alpha,1}(t;\lambda)$, when $\lambda = 2.0$, for $\alpha = 0.7$ (left plot) and $\alpha = 1.3$ (right plot).

The behaviour of the exponential terms $G_{\alpha}(t;\lambda)$ and $H_{\alpha}(t;\lambda)$ clearly depends on the location, in the complex plane, of their respective arguments, i.e. the singularities of $\mathcal{E}_{\alpha,\beta}(s;(-\mathrm{i})^{\alpha}\lambda)$.

As α varies, the first singularity $s^{\star}_1 = -\mathrm{i}\lambda^{1/\alpha}$ can just move up and down but it remains on the negative imaginary axis; thus, for a fixed $\lambda < 1$, $G_{\alpha}(t;\lambda)$ presents persisting oscillations with increasing frequency as α increases from 0 to 2 as one can clearly see from Figure 4.

On the contrary, when $\lambda > 1$ the frequency of the oscillations of $G_{\alpha}(t;\lambda)$ decreases as the fractional order α increases (see Figure 5) and very highly oscillatory frequencies can be clearly associated to small values of α.

The second singularity $s^{\star}_2 = -\mathrm{i}\lambda^{1/\alpha}\mathrm{e}^{\mathrm{i}2\pi/\alpha}$ appears only when $\alpha > 4/3$ and moves from the real negative axis to the positive imaginary axis as α increases from $4/3$ to 2 (its location in the complex plane is indicated in Figure 6, together with that of $s^{\star}_1$). $H_{\alpha}(t;\lambda)$ presents therefore damped oscillations when α is close to $4/3$ which tend to become more sustained when α is close to 2. The behaviour of $H_{\alpha}(t;\lambda)$ is illustrated in Figure 7.

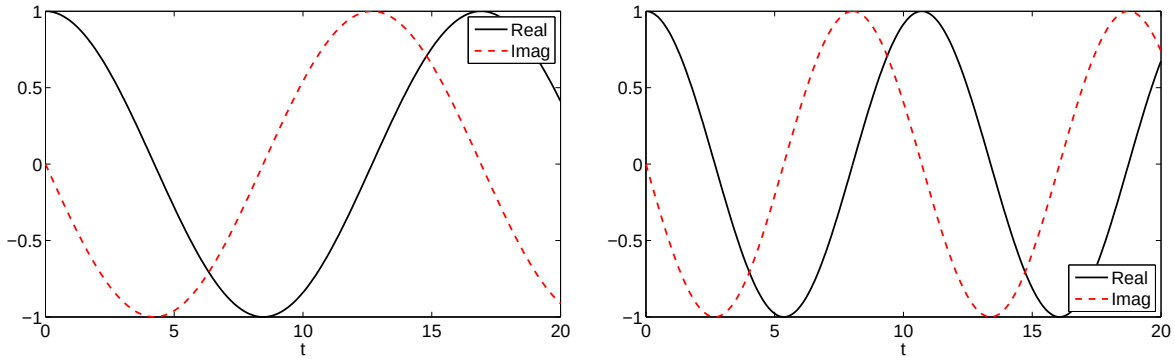

Figure 4: Real and imaginary parts of $G_\alpha(t;\lambda)$, when $\lambda = 0.5$, for $\alpha = 0.7$ (left plot) and $\alpha = 1.3$ (right plot).

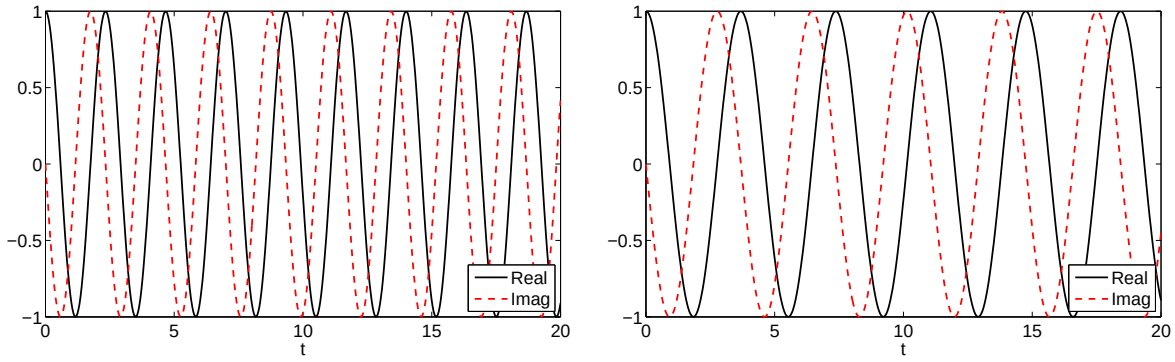

Figure 5: Real and imaginary parts of $G_\alpha(t;\lambda)$, when $\lambda = 2.0$, for $\alpha = 0.7$ (left plot) and $\alpha = 1.3$ (right plot).

The behaviour of the whole function $e_{\alpha,\beta}(t;(-\mathrm{i})^\alpha\lambda)$ is presented in Figure 8 for $\lambda > 1$ (when $\lambda < 1$ it is similar); it is hence given by regular and oscillating functions and, obviously, it will preserve the persisting oscillating character of $G_\alpha(t;\lambda)$ to which the damped functions $F_{\alpha,\beta}(t;\lambda)$ and $H_\alpha(t;\lambda)$ are added.

It is thus clear that the overall dynamics of $e_{\alpha,\beta}(t;(-\mathrm{i})^\alpha\lambda)$ bears the different behaviour of the terms $F_{\alpha,\beta}, G_\alpha$ and H_α: it is thus the highly oscillating character of $G_\alpha(t;\lambda)$ (and in some cases of $H_\alpha(t;\lambda)$) to make extremely difficult its approximation.

On the other side we must recognize that the evaluation of the scalar functions $G_\alpha(t;\lambda)$ and $H_\alpha(t;\lambda)$ does not present any particular difficulty since these are just elementary functions. Contrarily the evaluation of $F_{\alpha,\beta}(t;\lambda)$ turns out to be more challenging since only integral formulations are available; as a matter of fact, it is $F_{\alpha,\beta}(t;\lambda)$ which absorbs the non-locality of the ML function and the resulting computational difficulty although, due to its regularity, the approximation of $F_{\alpha,\beta}(t;\lambda)$ appears easier.

4.2 Evaluation on matrix arguments

By assuming that the matrix argument A has a real positive spectrum (as it is reasonable within the application discussed in this paper), the result of Theorem 4.2 can be generalized in a straightforward way to the matrix function $e_{\alpha,\beta}(t;(-\mathrm{i})^\alpha A)$. Then the solution of the TFSE (2) (with $b = 0$ just for ease of presentation) can be split as

$$y(t) = z_F(t) + \frac{1}{\alpha}\left(z_G(t) + \varphi(\alpha)^{1-\beta} z_H(t)\right), \tag{8}$$

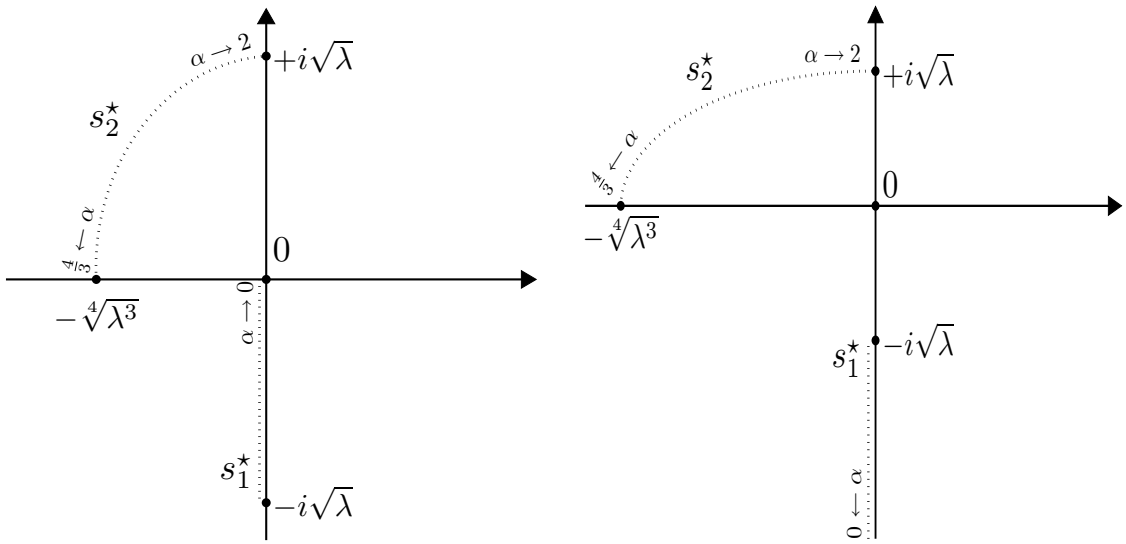

Figure 6: Location (dot lines) in the complex plane of the singularities $s_1^\star$ and $s_2^\star$ of $\mathcal{E}_{\alpha,\beta}(s;(-\mathrm{i})^\alpha\lambda)$ with respect to α when $\lambda < 1$ (left) and $\lambda > 1$ (right).

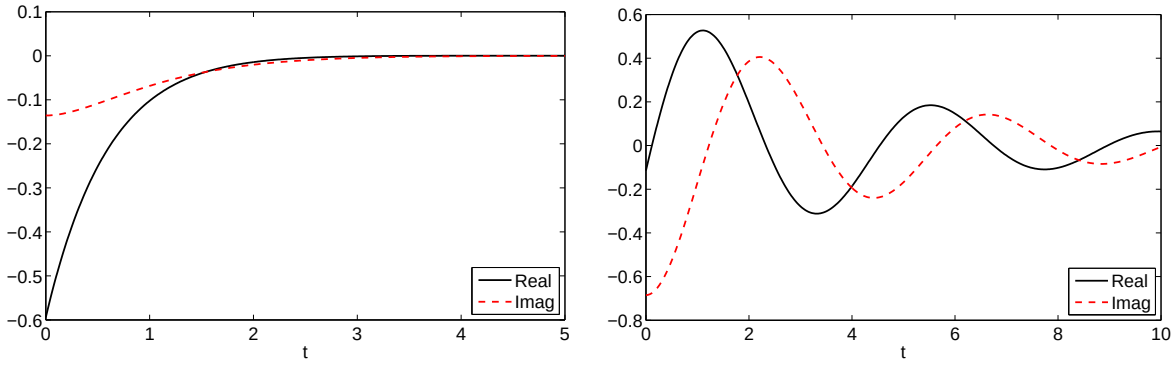

Figure 7: Real and imaginary parts of $H_\alpha(t;\lambda)$, when $\lambda = 2.0$, for $\alpha = 1.4$ (left plot) and $\alpha = 1.9$ (right plot).

where

$$z_F(t) = \begin{cases} F_{\alpha,1}(t;A)y_0 & \text{if } 0 < \alpha \le 1 \\ F_{\alpha,1}(t;A)y_0 + F_{\alpha,2}(t;A)y_0' & \text{if } 1 < \alpha < 2 \end{cases},$$

$$z_G(t) = \begin{cases} G_\alpha(t;A)y_0 & \text{if } 0 < \alpha \le 1 \\ G_\alpha(t;A)\left(y_0 + \mathrm{i}A^{-\frac{1}{\alpha}}y_0'\right) & \text{if } 1 < \alpha < 2 \end{cases},$$

and

$$z_H(t) = \begin{cases} 0 & \text{if } 0 < \alpha \le \frac{4}{3} \\ H_\alpha(t;A)\left(\frac{\mathrm{i}}{\varphi(\alpha)}A^{-\frac{1}{\alpha}}y_0 + y_0'\right) & \text{if } \frac{4}{3} < \alpha < 2 \end{cases}.$$

For the computation of the matrix functions in the various terms $z_F(t)$, $z_G(t)$ and $z_H(t)$, Krylov subspace methods appear clearly the most suitable because of the large size and sparsity of the matrix A. For the function $F_{\alpha,\beta}(t;A)$ a small Krylov subspace is in fact sufficient to obtain a good approximation; one can actually verify this from Figure 9 which reports, as α varies, the minimum size of the Krylov subspace necessary to obtain a relative error less than 10^{-8}.

As one can readily observe, the dimension of the Krylov subspace necessary to approximate $F_{\alpha,\beta}(t;A)$ within a given accuracy does not depend in a decisive way on α and t. Neither the size of A seems to have a relevant impact on convergence, at least according

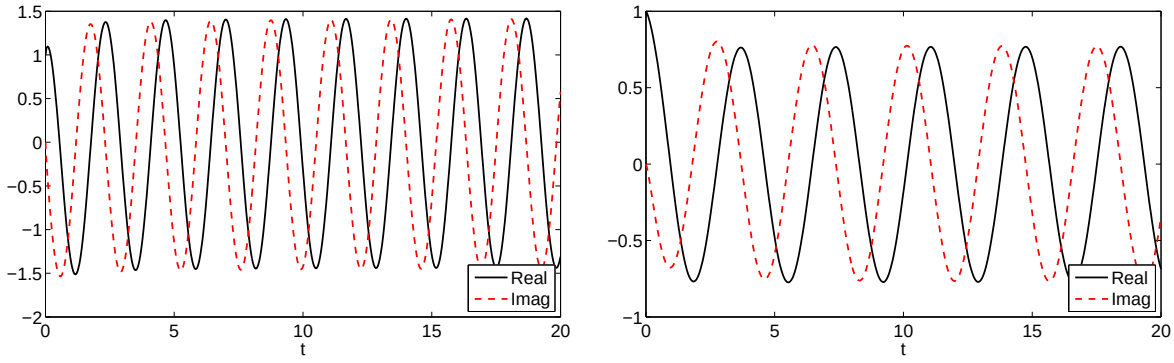

Figure 8: Real and imaginary parts of $e_{\alpha,1}(t;\lambda)$, when $\lambda = 2.0$, for $\alpha = 0.7$ (left plot) and $\alpha = 1.3$ (right plot).

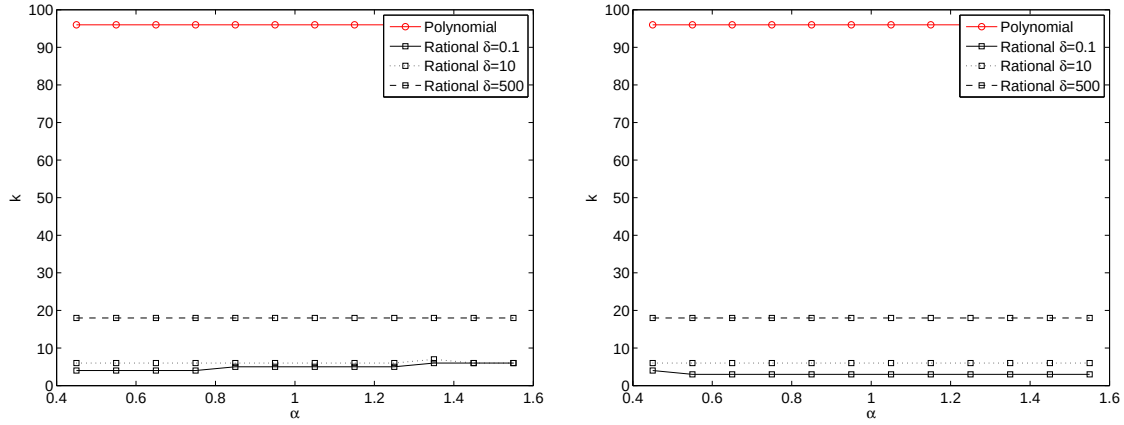

Figure 9: Minimum dimension of the Krylov subspace in order to approximate $F_{\alpha,1}(t;A)$ with a relative error equal to 10^{-8} at $t = 1$ (left) and $t = 100$ (right) for $N = 4900$.

to many other numerical tests not reported here for brevity's sake. Anyway the rational SIKM provides better results than the polynomial SKM method, especially for suitable values of the shift parameter δ, but it is worthwhile to remark that a fine tuning of δ does not offer substantial improvements in this context. The convergence properties of the different methods will be however investigated more in-depth, under a theoretical point of view, in the subsequent section.

More difficulties are expected for the evaluation of $z_G(t)$ (and of $z_H(t)$ when α is close to 2). Indeed, since the subspace Krylov approximations can be viewed as interpolations, a function with high-frequency oscillations demands for a large number of interpolating nodes in order to be approximated in acceptable way; contrarily, for more regular functions it can be expected that few information are sufficient to provide an accurate enough approximation. This is an intuitive consequence of the Nyquist-Shannon sampling theorem but can also be reasoned on the basis of more classic results in approximation theory.

So, especially when α is small, the frequency of the oscillations in $G_\alpha(t;A)$ can be so high to demand for a very large amount of information to approximate the function in a satisfactory way; the situation gets even worse on large, or even moderately large, intervals $[0,T]$, and in most cases the convergence of Krylov subspace methods can not be achieved in a reasonable number of iterations (memory requirements forced us to set at 500 the maximum size of the Krylov subspaces).

This problem can be however partially bypassed since $G_\alpha(t;A)$ and $H_\alpha(t;A)$ are ex-

ponential functions and hence, as already proposed in [12], it is possible to split the computation in a step-by-step way. Indeed, for any step-size $h > 0$ it is

$$z_G(t) = G_\alpha(h; A) z_G(t-h), \quad z_H(t) = H_\alpha(h; A) z_H(t-h),$$

thus allowing to consider just exponential on considerably shorter time-intervals $[0, h]$ in which the computation is more affordable.

As we can see from Figure 10 it is necessary to use a reasonable small step-size $h > 0$ in order to assure convergence of the Krylov subspace methods in a reasonable number of iterations (the flat lines in the first part of the α interval denote that no convergence is achieved in the maximum of 500 iterations).

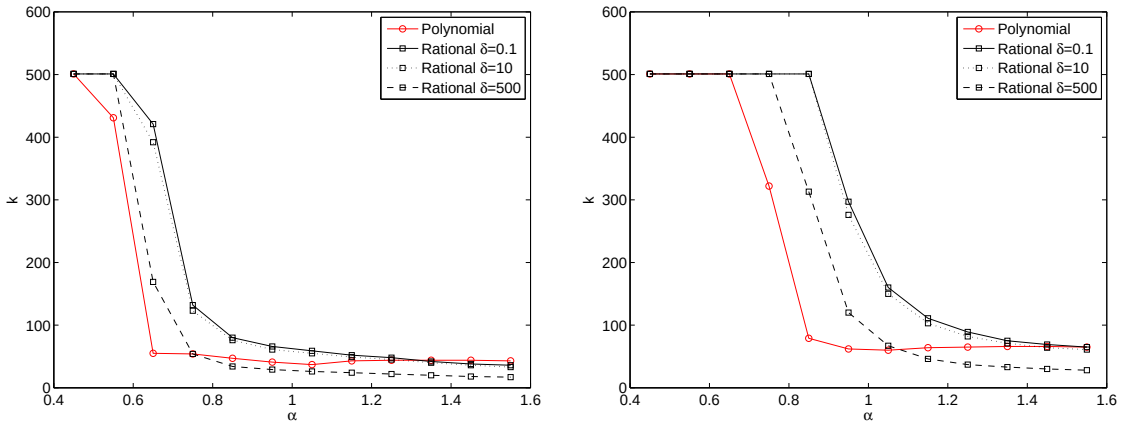

Figure 10: Minimum dimension of the Krylov subspace for approximating $\exp(-\mathrm{i}hA^{1/\alpha})$ with a relative error equal to 10^{-8} for $h = 10^{-5}$ (left) and $h = 10^{-3}$ (right) for $N = 4900$.

Convergence for $\exp\big(-\mathrm{i}hA^{1/\alpha}\big)$ still however remains a serious issue with moderate values of h, especially when $\alpha < 1$.

The situation for $z_H(t)$ is similar since it involves the exponential with matrix argument $-\varphi(\alpha)\mathrm{i}A^{1/\alpha}$. We however omit to discuss it explicitly since $z_H(t)$ is of less interest because it appears only for α sufficiently large while TFSEs are more interesting when α is close to 1.

4.3 Numerical computation of $F_{\alpha,\beta}(t; \lambda)$

Unlike the functions $G_\alpha(t; \lambda)$ and $H_\alpha(t; \lambda)$ which are expressed in terms of elementary functions, the evaluation of $F_{\alpha,\beta}(t; \lambda)$ is more challenging since only its integral representation is known.

The function $F_{\alpha,\beta}(t; \lambda)$ can be numerically evaluated, in the scalar case, by applying a quadrature rule to the integral in (6); precisely, the contour $\mathcal{H}_\gamma$ needs to be replaced with a contour suitably selected in order to minimize errors and obtain an accuracy as close as possible to the machine precision. An effective procedure for the selection of the contour is investigated in [38, 39] and applied to the ML function in [40, 36].

5 Convergence results

The convergence analysis for Krylov subspace approximations is fundamental to relate the error behaviour and the dimension of the projection spaces. Concerning the problems here considered, for $\alpha < 1$ this analysis has been deepened in the recent paper [12]. Thus

for such cases we refer the reader to that paper. The results given below want to extend the analysis to $1 < \alpha < 2$.

We address the convergence analysis for the SIKM, thus the Krylov subspace is $\mathbb{K} = \mathcal{K}_{m+1}(Z, v)$ for $Z = (\delta I + A)^{-1}$ and $m \geq 1$. In general the SIKM can be realized also following the general definition of the rational Krylov methods, that is, $f(A)v \approx f(\bar{A})Pv$, where $\bar{A} = PAP$ with P being the orthogonal projection onto $\mathbb{K}$. In practice, the two SIKM approximations give analogous results. For clarity of exposition, in performing our convergence analysis we will refer to the latter formulation. Moreover, we recall that we assume that $\sigma(A) \subset [a, +\infty[$ for some $a > 0$.

To facilitate the reading of the paper, the proofs of the propositions below are collected in Appendix.

The following results illustrate the convergence of the rational SIKM for the computation of $E_{\alpha,\beta}((-\mathrm{i}t)^\alpha A)v$.

Proposition 5.1. *Let $m \geq 1$ and $t > 0$; then, for $\beta = 1, 2$ and for every $\delta \geq a$, there is a constant $C(\delta)$, depending only on δ, such that*

$$\left\| E_{\alpha,\beta}((-\mathrm{i}t)^\alpha A)v - E_{\alpha,\beta}((-\mathrm{i}t)^\alpha \overline{A})v \right\| \leq C(\delta) \frac{\exp(ta^{\frac{1}{\alpha}}) \left\| Av \right\|}{a} m^{-c(\alpha)},$$

where $c(\alpha) = \frac{1}{3}$ if $1 < \alpha < \frac{8}{5}$ while $c(\alpha) = \frac{2(\alpha-1)}{\alpha+2}$ if $\frac{8}{5} \leq \alpha \leq 2$.

The previous Proposition says that we may have an $O(\ m^{-c(\alpha)})$ error with $c(\alpha)$ depending only on α. Thus it predicts, in the worst case, a sublinear convergence for the SIKM, like it may occur in solving the integer-derivative Schrödinger equation as well as dealing with the wave equation (see [41, 42, 43, 44]). The rate of convergence may improve as α grows and this is confirmed by the numerical experiments reported in the previous sections.

Yet, we observed that in practice the bound is often pessimistic. Indeed it is rather qualitative. Anyhow, it shows the mesh independence of the "rate of convergence" of the method, even if the bound depends on $\left\| Av \right\|$.

We point out that the choice $\delta \geq a$ is not restrictive since a can be taken as any value in the interval $(0, \lambda_{\min}]$ with $\lambda_{\min}$ the minimum eigenvalue of A. From the theoretical analysis (see Appendix) it seems that $\delta = a$ could be a "good" choice. Yet, in several numerical experiments we did not find substantial differences varying δ. We must also point out that the conditioning of $(\delta I + A)$ (and so the accuracy of the method) improves as δ increases.

In order to compute the oscillatory part $z_G(t)$ in $e_{\alpha,\beta}((-\mathrm{i}t)^\alpha A)v$, that is $A^{\frac{1-\beta}{\alpha}} \exp(-\mathrm{i}tA^{\frac{1}{\alpha}})v$, $\beta \in \{1, 2\}$, exploiting the fact that

$$\lim_{t \to 0^+} (\exp(-\mathrm{i}tA^{\frac{1}{\alpha}})v - \exp(-\mathrm{i}t\overline{A}^{\frac{1}{\alpha}})v) = 0,$$

the step-by-step strategy discussed in Section 4 appears as the most reasonable. Concerning the convergence (with respect to m) of this approach, the following statements hold.

Proposition 5.2. *The upper bound stated in Proposition 5.1 holds true even for* $\left\| \exp(-\mathrm{i}tA^{\frac{1}{\alpha}})v - \exp(-\mathrm{i}t\overline{A}^{\frac{1}{\alpha}})v \right\|$.

Proposition 5.3. *Let $1 < \alpha < 2$. Then for every $\delta > 0$ there is a sequence of positive scalars $\{\eta_m\}$, with $\eta_m \to 0$ (as $m \to \infty$), such that it holds that*

$$\left\| A^{-\frac{1}{\alpha}}v - \overline{A}^{-\frac{1}{\alpha}}v \right\| \leq \eta_m \left\| v \right\|.$$

We point out that, as it was shown in [45] (cf. also [46]), if $\sigma(A) \subset [a, b]$ then taking $\delta = \sqrt{ab}$, we get $\eta_m = O(\exp(-2m\sqrt[4]{a/b}))$. We recall that the error for the polynomial SKM is $O(\exp(-2m\sqrt{a/b}))$ (see [47]). We notice that an alternative "optimal" choice of δ was proposed in [45] which can make the rate of convergence independent of the spectrum size. See [32] for a restarted version of the SIKM.

We observe that the numerical computation of $\exp(-\mathrm{i}tA^{\frac{1}{\alpha}})v$, namely the solution of

$$y'(t) = -\mathrm{i}A^{\frac{1}{\alpha}}y(t),\ y(0) = v,$$

could be addressed even by any classical solver. Yet, also in this case the application of functions of $\mathrm{i}A^{\frac{1}{\alpha}}$ is required.

6 Numerical experiments

For all the experiments presented throughout the various sections of the paper, we have considered Eq. (1) into a two-dimensional square domain $\Omega = [-2, 2] \times [-2, 2]$. The potential $V(x)$ is assumed to be zero inside the interior of the subdomain $\Omega_p = [-1, 1] \times [-1, 1]$ and constant outside, namely $V(x) = 0$ for $x \in int(\Omega_p)$ and $V(x) = 10$ when $x \in cl(\Omega/\Omega_p)$. The initial distribution at the time $t = 0$ is of Gaussian type, i.e. $\psi(0, x) = e^{-|x|^2/2}$, and all the constants are normalized according to $\hbar = T_p = \hat{m} = 1$.

The Laplacian ∇_x^2 has been discretized by means of classic second order central differences, on equispaced mesh-grids, in order to recast Eq. (1) as the linear system of FDEs (2). For simplicity, in all the tests we have used $y_0 = y_0'$.

In this Section we aim to show the accuracy which can be obtained with the approach discussed in the previous sections and provide a hint of the corresponding involved computational effort. Since we are interested in studying the dependence of the attainable accuracy on the order α and the size of the problem, we approximate the vectors in (3) by using the split in (8) for different values of α and of matrix dimensions $N \times N$ (this corresponds to different discretizations of the Laplacian in (1)).

To tune the involved parameters we use the results from the numerical tests presented before: for the term z_F, for example, Figure 9 suggests to use the SIKM method with a tiny dimension m, say $m = 10$ with shift parameter $\delta = 0.1$. Indeed, this term can be computed in a very fast way, with a computational time usually under tenths of seconds; for this reason only the computational time for $z_G(t)$ will be reported.

According to Figure 10, for $z_G(t)$ we use SKM when $\alpha < 1$, with $m = 50$ and $h = 10^{-5}$, while when $\alpha > 1$ we apply the SIKM with $m = 50$, $\delta = 500$ and $h = 10^{-3}$.

As expected, the case $\alpha < 1$ is very difficult to treat: we chose to reduce the step h to accelerate the convergence of the Krylov subspace method: in this way a small space dimension suffices to get good accuracy. However, thousands of steps are needed to reach the final t value, with a very large global execution time. Nonetheless, the accuracy we reach on the approximation is very satisfactory and, if lower accuracies are required, lower execution time can be expected, as we can clearly observe from Table 1.

We can conclude that only a proper use of the Krylov subspace methods allows to reach the required accuracy in reasonable times. Indeed, a thorough application to $e_{\alpha,\beta}$ is wasteful, as shown in Figures 1-2, while the split in (8) allows to tackle each component in the most appropriate way, as to globally reach the required accuracy.

N	$\alpha = 0.7$	$\alpha = 0.9$	$\alpha = 1.1$	$\alpha = 1.3$
100	$3.4 \cdot 10^{-13}$ (37.3 sec.)	$2.5 \cdot 10^{-13}$ (52.3 sec.)	$2.7 \cdot 10^{-12}$ (0.7 sec.)	$9.9 \cdot 10^{-11}$ (0.6 sec.)
900	$1.3 \cdot 10^{-11}$ (379.2 sec.)	$1.0 \cdot 10^{-12}$ (372.7 sec.)	$2.1 \cdot 10^{-11}$ (4.6 sec.)	$4.3 \cdot 10^{-9}$ (4.3 sec.)
2500	$2.3 \cdot 10^{-6}$ (20192 sec.)	$2.5 \cdot 10^{-11}$ (1716 sec.)	$5.1 \cdot 10^{-10}$ (30.5 sec.)	$1.1 \cdot 10^{-8}$ (30.2 sec.)

Table 1: Relative errors in computing the solution (3) at $t = 0.1$ by using the split in (8) for different values of α and of matrix dimensions $N \times N$. The CPU time required for z_G is in parentheses (the CPU time for the other terms is negligible).

Appendix A Proofs of the convergence results

For the proofs of the convergence results we use an integral formulation of the ML function based on the Hankel representation on the contour $Q(\varepsilon, \mu)$ consisting of the following three parts:

1. $\arg \xi = -\mu$, $|\xi| > \varepsilon$,
2. $-\mu \leq \arg \xi \leq \mu, |\xi| = \varepsilon$,
3. $\arg \xi = \mu$, $|\xi| > \varepsilon$,

where for $0 < \alpha < 2$, it is $\frac{\alpha\pi}{2} < \mu \leq \min[\pi, \alpha\pi]$ and $\varepsilon > 0$.

The contour $Q(\varepsilon, \mu)$ is oriented in such a way that $\arg \xi$ is non-decreasing. It divides the complex plane into a left domain $G_-(\varepsilon, \mu)$ and a right domain $G_+(\varepsilon, \mu)$. The choice $\mu = \pi$ is allowed and $G_+(\varepsilon, \pi)$ becomes $\mathbb{C}$ excluding the circle $|z| < \varepsilon$ and the line $|\arg z| = \pi$. The following representation [28, Theorem 1.1] holds for $z \in G_+(\varepsilon, \mu)$:

$$e_{\alpha,\beta}(t^\alpha z) = (-\mathrm{i})^{1-\beta} z^{\frac{1-\beta}{\alpha}} \frac{\exp(t z^{\frac{1}{\alpha}})}{\alpha} + \frac{1}{2\alpha\pi\mathrm{i}} \int_{Q(\varepsilon,\mu)} \exp(-t\xi^{\frac{1}{\alpha}}) \xi^{\frac{1-\beta}{\alpha}} (\xi - z)^{-1} d\xi.$$

The extension of the previous formulae to our matrices is obvious, recalling also that in our case $A^{\frac{1}{\alpha}}$ is defined through its Schur decomposition. We point out that we are interested to give convergence results which hold for every discretization introduced. This motivates to assume $\sigma(A) \subset [a, +\infty)$, $a > 0$.

We recall that (see [28, Theorem 1.5]) there is a constant C such that for every $u \in G_+(\varepsilon, \mu)$ it holds that

$$|E_{\alpha,\beta}(u)| \leq C \left((1 + |u|)^{\frac{1-\beta}{\alpha}} \exp(\Re u^{\frac{1}{\alpha}}) + (1 + |u|)^{-1} \right). \tag{9}$$

From now on, for $\lambda (\neq 0) \notin \sigma(A) \cup \sigma(\overline{A})$ let us set

$$D(\lambda) = (\lambda I - A)^{-1} - (\lambda I - \overline{A})^{-1} P \tag{10}$$

and $\Phi(\varkappa) = \varkappa + \sqrt{\varkappa^2 - 1}$, $\varkappa \geq 1$.

Proof. of Proposition 5.1.

At first assume that $\alpha < 8/5$. Consider the positively oriented (counterclockwise) contour Γ consisting of the following parts:

1) $\Gamma_{2+} = \left\{ \lambda \in \mathbb{C} : \lambda = ar \exp(\mathrm{i}\frac{\pi}{6r}) \text{ for } 1 \leq r < +\infty \right\}$;

2) $\Gamma_1 = \left\{ \lambda \in \mathbb{C} : \lambda = a(\sqrt{3} + \mathrm{i}\rho)/2, -1 \leq \rho \leq 1 \right\}$;

3) $\Gamma_{2-} = \left\{\lambda \in \mathbb{C} : \lambda = ar\exp(-\mathrm{i}\frac{\pi}{6r}) \text{ for } 1 \leq r < +\infty\right\}$.

For the sake of simplicity we set $\Gamma_2 = \Gamma_{2+} \cup \Gamma_{2-}$.

Owing to (9), we notice that, for $\beta = 1, 2$, the function $E_{\alpha,\beta}((-\mathrm{i}t)^\alpha\lambda)$ is continuous and uniformly bounded on Γ and it is analytic in the right-sided domain (in $\mathbb{C}_+$) surrounded by Γ. Moreover from (9), for every $t > 0$, we have

$$|E_{\alpha,\beta}((-\mathrm{i}t)^\alpha\lambda)| \leq C\left((1+|t^\alpha\lambda|)^{-\frac{\beta-1}{\alpha}}\exp(ta^{\frac{1}{\alpha}}) + (1+|t^\alpha\lambda|)^{-1}\right)$$

and so

$$|E_{\alpha,\beta}((-\mathrm{i}t)^\alpha\lambda)| \leq C\exp(ta^{\frac{1}{\alpha}}), \text{ for } \lambda \in \Gamma.$$

Employing the Dunford-Taylor representation theorem and applying Lemma 9 in [12] we obtain

$$\left(E_{\alpha,\beta}\left((-\mathrm{i}t)^\alpha A\right) - E_{\alpha,\beta}\left((-\mathrm{i}t)^\alpha\overline{A}\right)\right)v = \frac{1}{2\pi\mathrm{i}}\int_\Gamma \frac{E_{\alpha,\beta}((-\mathrm{i}t)^\alpha\lambda)}{\lambda}\frac{D(\lambda)p_m(Z)}{p_m((\lambda+\delta)^{-1})}Avd\lambda$$

for every $p_m \in \Pi_m$, where Π_m denotes the set of all algebraic polynomials of degree at most m. Therefore

$$\left\|(E_{\alpha,\beta}((-\mathrm{i}t)^\alpha A) - E_{\alpha,\beta}((-\mathrm{i}t)^\alpha\overline{A}))v\right\| \leq \frac{I_1+I_2}{2\pi}, \tag{11}$$

where for $k = 1, 2$,

$$I_k = \left\|\int_{\Gamma_k}\frac{E_{\alpha,\beta}((-\mathrm{i}t)^\alpha\lambda)}{\lambda}\frac{D(\lambda)p_m(Z)}{p_m((\lambda+\delta)^{-1})}Avd\lambda\right\|. \tag{12}$$

For $\lambda \in \Gamma_1$, referring to (10), it holds that

$$\|D(\lambda)\| \leq C/a.$$

In order to apply Lemmas $10-13$ in [12], setting $\eta = \delta/a$ we realize that

$$\omega(\lambda) = \frac{\delta + a + |\lambda - a|}{|\lambda+\delta|} \geq \frac{2(\eta+1)+|\rho|}{\sqrt{\rho^2 + (2\eta+\sqrt{3})^2}} \geq \frac{2(\eta+1)}{2\eta+\sqrt{3}}.$$

Therefore

$$\Phi(\omega(\lambda))^{-1} \leq q(\eta) = \frac{2\eta+\sqrt{3}}{2(\eta+1)+\sqrt{1+2\eta(2-\sqrt{3})}}.$$

So, by Lemmas $10-13$ in [12] we have

$$I_1 \leq C\frac{\exp(ta^{\frac{1}{\alpha}})\,\|Av\|}{a}q(\eta)^m. \tag{13}$$

Now we consider $\lambda \in \Gamma_2$. At first we point out that

$$\left|\frac{E_{\alpha,\beta}((-\mathrm{i}t)^\alpha\lambda)}{\lambda}\right| \leq C\frac{\exp(ta^{\frac{1}{\alpha}})}{ar}$$

and moreover that

$$|d\lambda| = a\left(\sqrt{1+\left(\frac{\pi}{6}\right)^2 r^{-2}}\right)\,\mathrm{d}r. \tag{14}$$

In this case

$$\omega(\lambda) = \frac{\delta + a + |\lambda - a|}{|\lambda + \delta|} \geq \frac{\eta + r}{\sqrt{\eta^2 + r^2 + 2r\eta\cos(\pi/6r)}} \equiv g(r). \tag{15}$$

Moreover, for $L = A/a$ and $\overline{L} = \overline{A}/a$ we have

$$D(\lambda) = \frac{1}{a}\left(\left(r\exp\left(\pm i\frac{\pi}{6r}\right)I - L\right)^{-1} - \left(r\exp\left(\pm i\frac{\pi}{6r}\right)I - \overline{L}\right)^{-1}\right). \tag{16}$$

Thus, by (14) and (16), employing Lemmas 9, 10, 13 in [12], applying Schwarz's inequality, by simple computation we get

$$I_2 \leq C\frac{\exp(ta^{\frac{1}{\alpha}})\,\|Av\|}{a}\left(\int_1^\infty r^{-2}\Phi(g(r))^{-2m}\,\mathrm{d}r\right)^{\frac{1}{2}} \tag{17}$$

where

$$\Phi(g(r)) = \frac{\eta + r + \sqrt{2r\eta(1-\cos\frac{\pi}{6r})}}{\sqrt{\eta^2 + r^2 + 2r\eta\cos\frac{\pi}{6r}}}.$$

By direct computation, one realizes that

$$\Phi(g(r)) \geq 1 + \frac{\sqrt{2r\eta(1-\cos\frac{\pi}{6r})}}{\sqrt{\eta^2 + r^2 + 2r\eta\cos\frac{\pi}{6r}}} \geq 1 + \frac{\sqrt{\eta}}{4\sqrt{r}(r+\eta)}$$

and we get

$$\Phi(g(r))^{-1} \leq 1 - \frac{\sqrt{\eta}}{4\sqrt{r}(r+\eta) + \sqrt{\eta}} \leq \exp\left(-\frac{1}{8r\sqrt{\eta r} + 1}\right)$$

Therefore we have

$$\int_1^\infty r^{-2}\Phi(g(r))^{-2m}\,\mathrm{d}r \leq \int_1^\infty r^{-2}\exp\left(\frac{-2m}{(1+8\sqrt{\eta})r^{3/2}}\right)\,\mathrm{d}r.$$

Using formulae (13.2.1) and (13.1.5) in [48], one verifies that

$$\int_1^\infty r^{-2}\Phi(g(r))^{-2m}\,\mathrm{d}r \leq C\left(\frac{1+8\sqrt{\eta}}{2m}\right)^{\frac{2}{3}}. \tag{18}$$

Thus by (18), collecting (17) and (13) we get the bound

$$\left\|E_{\alpha,\beta}((-\mathrm{i}t)^\alpha A)v - E_{\alpha,\beta}((-\mathrm{i}t)^\alpha\overline{A})v\right\| \leq C\frac{\exp(ta^{\frac{1}{\alpha}})\,\|Av\|}{a}\left(q(\eta)^m + C(\delta)m^{-c(\alpha)}\right) \tag{19}$$

for some $C(\delta)$ depending on δ and $c(\alpha) = 1/3$.

Now let $8/5 \leq \alpha \leq 2$; consider the positively oriented contour Γ with Γ_1 as before and $\Gamma_2 = \Gamma_{2+} \cup \Gamma_{2-}$ for $\Gamma_{2\pm} = \left\{\lambda \in \mathbb{C} : \lambda = ar\exp(\pm\mathrm{i}\frac{\pi r^{-\frac{1}{\alpha}}}{6}) \text{ for } r \geq 1\right\}$.

Again we find that, for $\beta = 1, 2$, the function $E_{\alpha,\beta}((-\mathrm{i}t)^\alpha\lambda)$ is continuous and uniformly bounded on Γ and it is analytic in the right-sided set (in $\mathbb{C}_+$) surrounded by Γ. Proceeding as before we get (11), (12) and (13). For $\lambda \in \Gamma_2$ we realize that

$$|d\lambda| = a\left(\sqrt{1 + \left(\frac{\pi}{6\alpha}\right)^2 r^{-\frac{2}{\alpha}}}\right)\,\mathrm{d}r$$

and that (15), (17) and (18) still hold. Now, observing that

$$\|D(\lambda)\| \leq \frac{Cr^{-1+\frac{1}{\alpha}}}{a},$$

by (14) and (16), employing Lemmas 9, 10, 13 in [12] we get

$$I_2 \leq C\frac{\exp(ta^{\frac{1}{\alpha}})\,\|Av\|}{a}\int_1^\infty r^{-2+\frac{1}{\alpha}}\Phi(g(r))^{-m}\,\mathrm{d}r.$$

Arguing as before we now obtain

$$\Phi(g(r))^{-1} \leq \exp\left(-\frac{1}{1+8\sqrt{\eta}r^{\frac{1}{\alpha}+\frac{1}{2}}}\right)$$

Therefore we have

$$\int_1^\infty r^{-2+\frac{1}{\alpha}}\Phi(g(r))^{-m}\,\mathrm{d}r \leq \int_1^\infty r^{-2+\frac{1}{\alpha}}\exp\left(\frac{-m}{(1+8\sqrt{\eta})r^{\frac{1}{\alpha}+\frac{1}{2}}}\right)\mathrm{d}r$$

and now one finds

$$\int_1^\infty r^{-2+\frac{1}{\alpha}}\Phi(g(r))^{-m}\,\mathrm{d}r \leq C\left(\frac{1+8\sqrt{\eta}}{m}\right)^{\frac{2(\alpha-1)}{\alpha+2}}.$$

Then we obtain again the bound (19) with $c(\alpha) = 2(\alpha-1)/(\alpha+2)$. The result is so proved. □ □

Proof. of Proposition 5.2. Let us reconsider the contours Γ introduced before and observe that the function $\exp(-\mathrm{i}t\lambda^{\frac{1}{\alpha}})$ is continuous and uniformly bounded on Γ and it is analytic in the right-sided domain surrounded by Γ. Thus proceeding as before, with the obvious changes, the bounds follow. □ □

Proof. of Proposition 5.3. We observe that, setting $\overline{Z} = (\delta I + \overline{A})^{-1} : \mathbb{K} \to \mathbb{K}$, we have

$$p_m(Z)v = p_m(\overline{Z})v,$$

for every $p_m \in \Pi_m$ and therefore

$$(A^{-\frac{1}{\alpha}} - \overline{A}^{-\frac{1}{\alpha}})v = (A^{-\frac{1}{\alpha}} - p_m(Z))v - (\overline{A}^{-\frac{1}{\alpha}} - p_m(\overline{Z}))v. \tag{20}$$

As it is well known the following Stieltjes representation holds

$$A^{-\frac{1}{\alpha}}v = \frac{\sin(\pi - \pi/\alpha)}{\pi}\int_0^{+\infty}\lambda^{-\frac{1}{\alpha}}(\lambda I + A)^{-1}v d\lambda.$$

Thus by a result given in [45], we know there is a sequence $\{p_m\}_m$ with $p_m \in \Pi_m$ and a sequence of positive scalars $\{\eta_m\}$, with $\eta_m \to 0$ as $m \to \infty$, such that for every Hermitian positive definite matrix A with $\sigma(A) \subset [a, +\infty]$ it is

$$\left\|(A^{-\frac{1}{\alpha}} - p_m((\delta I + A)^{-1}))v\right\| \leq 2\eta_m \|v\|.$$

Applying this to (20) the statement follows. □ □

References

[1] N. Laskin, Fractional quantum mechanics and Lévy path integrals, Physics Letters A 268 (4-6) (2000) 298–305.

[2] M. Naber, Time fractional Schrödinger equation, J. Math. Phys. 45 (8) (2004) 3339–3352.

[3] K. Diethelm, The analysis of fractional differential equations, Vol. 2004 of Lecture Notes in Mathematics, Springer-Verlag, Berlin, 2010.

[4] B. Al-Saqabi, L. Boyadjiev, Y. Luchko, Comments on employing the Riesz-Feller derivative in the Schrödinger equation, Eur. Phys. J. Special Topics 222 (8) (2013) 1779–1794.

[5] A. Ashyralyev, B. Hicdurmaz, On the numerical solution of fractional Schrödinger differential equations with the Dirichlet condition, Int. J. Comput. Math. 89 (13-14) (2012) 1927–1936.

[6] A. Ashyralyev, B. Hicdurmaz, A note on the numerical solution of fractional Schrödinger differential equations, AIP Conference Proceedings 1470 (1) (2012) 92–94.

[7] B. Hicdurmaz, A. Ashyralyev, A stable numerical method for multidimensional time fractional Schrödinger equations, Comput. Math. Appl. 72 (6) (2016) 1703–1713.

[8] A. H. Bhrawy, M. A. Abdelkawy, A fully spectral collocation approximation for multidimensional fractional Schrödinger equations, J. Comput. Phys. 294 (2015) 462–483.

[9] Q. Liu, F. Zeng, C. Li, Finite difference method for time-space-fractional Schrödinger equation, Int. J. Comput. Math. 92 (7) (2015) 1439–1451.

[10] B. N. Narahari Achar, B. T. Yale, J. W. Hanneken, Time fractional Schrödinger equation revisited, Advances in Mathematical Physics 2013 (290216) (2013) 1.

[11] L. Wei, X. Zhang, S. Kumar, A. Yildirim, A numerical study based on an implicit fully discrete local discontinuous Galerkin method for the time-fractional coupled Schrödinger system, Comput. Math. Appl. 64 (8) (2012) 2603–2615.

[12] R. Garrappa, I. Moret, M. Popolizio, Solving the time-fractional Schrödinger equation by Krylov projection methods, J. Comput. Phys. 293 (2015) 115–134.

[13] N. Del Buono, L. Lopez, R. Peluso, Computation of the exponential of large sparse skew-symmetric matrices, SIAM J. Sci. Comput. 27 (1) (2005) 278–293.

[14] L. Lopez, V. Simoncini, Preserving geometric properties of the exponential matrix by block Krylov subspace methods, BIT 46 (4) (2006) 813–830.

[15] E. Celledoni, I. Moret, A Krylov projection method for systems of ODEs, Appl. Numer. Math. 24 (1997) 365–378.

[16] M. Hochbruck, C. Lubich, H. Selhofer, Exponential integrators for large systems of differential equations, SIAM J. Sci. Comput. 19 (5) (1998) 1552–1574.

[17] N. Del Buono, L. Lopez, A survey on methods for computing matrix exponentials in numerical schemes for ODEs, in: Computational science—ICCS 2003. Part II, Vol. 2658 of Lecture Notes in Comput. Sci., Springer, Berlin, 2003, pp. 111–120.

[18] M. P. Calvo, C. Palencia, A class of explicit multistep exponential integrators for semilinear problems, Numer. Math. 102 (3) (2006) 367–381.

[19] M. Hochbruck, A. Ostermann, Exponential integrators, Acta Numer. 19 (2010) 209–286.

[20] M. Hochbruck, A. Ostermann, Exponential multistep methods of Adams-type, BIT 51 (4) (2011) 889–908.

[21] H. Berland, A. L. Islas, C. M. Schober, Conservation of phase space properties using exponential integrators on the cubic Schrödinger equation, J. Comput. Phys. 225 (1) (2007) 284–299.

[22] B. Cano, A. González-Pachón, Projected explicit Lawson methods for the integration of Schrödinger equation, Numer. Methods Partial Differential Equations 31 (1) (2015) 78–104.

[23] M. Hochbruck, C. Lubich, Exponential integrators for quantum-classical molecular dynamics, BIT 39 (4) (1999) 620–645.

[24] R. Garrappa, M. Popolizio, Generalized exponential time differencing methods for fractional order problems, Comput. Math. Appl. 62 (3) (2011) 876–890.

[25] M. Popolizio, A matrix approach for partial differential equations with Riesz space fractional derivatives, Eur. Phys. J. Special Topics 222 (8) (2013) 1975–1985.

[26] A. A. Kilbas, H. M. Srivastava, J. J. Trujillo, Theory and applications of fractional differential equations, Vol. 204 of North-Holland Mathematics Studies, Elsevier Science B.V., Amsterdam, 2006.

[27] F. Mainardi, Fractional calculus and waves in linear viscoelasticity, Imperial College Press, London, 2010.

[28] I. Podlubny, Fractional differential equations, Vol. 198 of Mathematics in Science and Engineering, Academic Press Inc., San Diego, CA, 1999.

[29] R. Gorenflo, A. Kilbas, F. Mainardi, S. Rogosin, Mittag–Leffler Functions, Related Topics and Applications, Springer Monographs in Mathematics, Springer, New York, 2014.

[30] N. J. Higham, Functions of matrices, Society for Industrial and Applied Mathematics (SIAM), Philadelphia, PA, 2008.

[31] I. Moret, P. Novati, On the convergence of Krylov subspace methods for matrix Mittag–Leffler functions, SIAM J. Numer. Anal. 49 (5) (2011) 2144–2164.

[32] I. Moret, M. Popolizio, The restarted shift-and-invert Krylov method for matrix functions, Numer. Linear Algebra Appl. 21 (1) (2014) 68–80.

[33] Y. Saad, Analysis of some Krylov subspace approximations to the matrix exponential operator, SIAM J. Numer. Anal. 29 (1) (1992) 209–228.

[34] I. Moret, P. Novati, RD-rational approximations of the matrix exponential, BIT 44 (3) (2004) 595–615.

[35] J. van den Eshof, M. Hochbruck, Preconditioning Lanczos approximations to the matrix exponential, SIAM J. Sci. Comput. 27 (4) (2006) 1438–1457.

[36] R. Garrappa, Numerical evaluation of two and three parameter Mittag-Leffler functions, SIAM J. Numer. Anal. 53 (3) (2015) 1350–1369.

[37] D. V. Widder, The Laplace Transform, Princeton Mathematical Series, v. 6, Princeton University Press, Princeton, N. J., 1941.

[38] J. A. C. Weideman, L. N. Trefethen, Parabolic and hyperbolic contours for computing the Bromwich integral, Math. Comp. 76 (259) (2007) 1341–1356.

[39] L. N. Trefethen, J. A. C. Weideman, The exponentially convergent trapezoidal rule, SIAM Rev. 56 (3) (2014) 385–458.

[40] R. Garrappa, M. Popolizio, Evaluation of generalized Mittag–Leffler functions on the real line, Advances in Computational Mathematics 39 (1) (2013) 205–225.

[41] V. Grimm, M. Hochbruck, Error analysis of exponential integrators for oscillatory second-order differential equations, J. Phys. A 39 (19) (2006) 5495–5507.

[42] V. Grimm, Resolvent Krylov subspace approximation to operator functions, BIT Numer. Math. 52 (2012) 639–659.

[43] I. Moret, A note on Krylov methods for fractional evolution problems, Numer. Funct. Anal. Optim. 34 (5) (2013) 539–556.

[44] I. Moret, Shift-and-invert Krylov methods for time-fractional wave equations, Numer. Funct. Anal. Optim. 36 (1) (2015) 86–103.

[45] I. Moret, Rational Lanczos approximations to the matrix square root and related functions, Numer. Linear Algebra Appl. 16 (6) (2009) 431–445.

[46] B. Beckermann, L. Reichel, Error estimation and evaluation of matrix functions via the Faber transform, SIAM J. Numer. Anal. 47 (2009) 3849–3883.

[47] V. Druskin, L. Knizhnerman, Extended Krylov subspaces: approximation of the matrix square root and related functions, SIAM. J. Matrix Anal. and Appl. 19 (3) (1998) 755–771.

[48] M. Abramowitz, I. A. Stegun, Handbook of mathematical functions with formulas, graphs, and mathematical tables, Vol. 55 of National Bureau of Standards Applied Mathematics Series, U.S. Department of Commerce, National Bureau of Standards, 1964.